Journal of Engineering Mathematics 17 (1983) 125–147

Slender channel theory in flow between two cylinders

P.G. DANIELS and P.M. EAGLES

Department of Mathematics, The City University, Northampton Square, London EC1V OHB, England

(Received August 1, 1982)

Summary

We consider high-Reynolds-number flow between a rotating inner circular cylinder and a fixed non-circular outer cylinder. The dimensionless gap width δ and the Reynolds number R are assumed to be related by $R\delta = \lambda$ where λ is a constant. Then the governing equations (to first approximation) are shown to be the classical boundary-layer equations, but with unusual boundary conditions. Numerical solutions and analytic approximations are found in various cases.

1. Introduction

There has been considerable interest recently in laminar, steady, high-Reynolds-number flows in slender channels. These channels are characterized by having a streamwise length scale of order R, where R is a Reynolds number. Introducing a streamwise co-ordinate x we set $X = x/R$ and assume the stream function $\psi = F(X, y)$ where y is a cross-channel co-ordinate. Then to a first approximation when R is large we obtain from the Navier-Stokes equations

$$F_{yyyy} = F_y F_{yyX} - F_X F_{yyy} \tag{1.1}$$

omitting terms of order R^{-2} and R^{-4}. This form of the stream function is consistent with the channel walls having equation $y = \pm H(X)$, for example, as described in Eagles and Smith [1]. The equation is the classical boundary layer equations, but derived with a different scaling.

In the case of channel flows this equation allows a number of interesting solutions, with separation and reattachment of the main flow in some cases. See, for example, Bodoia and Osterle [2], Paris and Whitaker [3], Blottner [4] and Plotkin [5].

In the present paper we consider the flow between a rotating inner cylinder of radius R_1 and angular velocity Ω_1 and a noncircular fixed outer cylinder. In a sense to be made more precise later, we assume that the gap-width δ in units of R_1 is small and the Reynolds number R is high, such that

$$R\delta = \lambda = \frac{\Omega d^2}{\nu} \tag{1.2}$$

where λ is considered to be O(1) as $R \to \infty$, $\delta \to 0$ in the first instance, though this

assumption is relaxed in Section 6. Under these assumptions and using suitable co-ordinates, we find the flow is governed to the first approximation by the slender-channel (i.e. boundary-layer) equations. However, the boundary condition on the inner rotating cylinder is different from that in channel theory, and the periodicity condition on the stream function and pressure introduces novel features.

There has been much previous work on a related problem, namely the flow between eccentric circular cylinders. DiPrima and Stuart [6] give an excellent summary of this work, and give a detailed expansion of the steady-state flow for small gap width δ. Their expansion is essentially for small δ, with the Taylor number held fixed, which amounts to $\delta \to 0$ with $R = O(\delta^{-1/2})$. DiPrima and Stuart's work was developed with the idea of considering the stability of the flows. In later papers (e.g. DiPrima and Stuart [7], Eagles et al. [8]), they introduced a relation $\delta^{1/2} = O(\varepsilon)$ between the small gap width δ and eccentricity ratio ε. We are able to show in Section 4 that our flow, expanded for δ small and $R = O(\delta^{-1/2})$ gives the first two terms of their expansion in the special case when our outer cylinder is approximately circular.

In the limit $\lambda \to 0$ our method, of course, gives just the equation $\psi_{\eta\eta\eta\eta} = 0$ where η is a cross-stream variable. This equation itself, with the moving inner wall and the variable gap gives flows of interest, with reversed flow in some cases and with relatively large pressure variations with the azimuthal angle. But these are all describable by earlier methods, at least for the eccentric cylinder case. As we increase $\lambda = R\delta$ these flows are modified by the nonlinear terms, the pressure variation becoming larger and the velocity profiles changing. But, unlike the case of channel flow, no drastic change in the *type* of flow is found to occur. However, it is possible that the stability properties of our flows *may* be considerably different from those examined by DiPrima and Stuart [6] as it is well known that the precise shape of the velocity profile is very important in these delicate stability calculations.

However, for the results we have obtained it is rather remarkable how little difference the nonlinear terms make to the velocity profiles. In the case of channel and tube flows with fixed boundaries the inclusion of the nonlinear terms makes a drastic difference. Here, however, all the essential features of the flow seem to be contained in the linear approximation, the role of the nonlinear terms being comparatively minor.

In Section 3 a description is given of some numerical solutions of the problem.

In Section 4 we consider briefly the solution as $\lambda \to 0$.

In Section 5 some analytic work is presented in the case where the smallest gap width is of order $\varepsilon\delta$, with $\varepsilon \to 0$ independently of δ. This enables us to make estimates of the extent of reversed flow and of points of attachment and separation, which fit well with the numerical results of Section 3.

In Section 6 some more analytic work for large values of λ is presented.

2. Formulation of the problem

Let r^*, θ, z^* be cylindrical polar co-ordinates. We consider flow between an inner cylinder $r^* = R_1$, rotating with angular velocity Ω_1 about its fixed axis, and a fixed outer cylinder to be described later (see Fig. 1).

Let d be the gap width at $\theta = 0$, let $r = r^*/d$ and let

$$R = \Omega_1 R_1 d/\nu$$

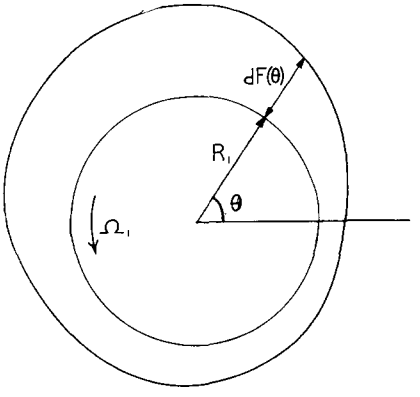

Fig. 1. Geometry and co-ordinates.

be the Reynolds number. Let velocities be made dimensionless by $\Omega_1 R_1$, and then if p is the appropriate dimensionless pressure the Navier-Stokes and continuity equations become, in the steady state

$$u\frac{\partial u}{\partial r}+\frac{v}{r}\frac{\partial u}{\partial \theta}-\frac{v^2}{r}=-\frac{\partial p}{\partial r}+\frac{1}{R}\left(\nabla^2 u-\frac{u}{r^2}-\frac{2}{r^2}\frac{\partial v}{\partial \theta}\right), \tag{2.1}$$

$$u\frac{\partial v}{\partial r}+\frac{v}{r}\frac{\partial v}{\partial \theta}+\frac{uv}{r}=-\frac{1}{r}\frac{\partial p}{\partial \theta}+\frac{1}{R}\left(\nabla^2 v+\frac{2}{r^2}\frac{\partial u}{\partial \theta}-\frac{v}{r^2}\right), \tag{2.2}$$

$$\frac{1}{r}\frac{\partial}{\partial r}(ru)+\frac{1}{r}\frac{\partial v}{\partial \theta}=0, \tag{2.3}$$

where

$$\nabla^2\equiv\frac{\partial^2}{\partial r^2}+\frac{1}{r}\frac{\partial}{\partial r}+\frac{1}{r^2}\frac{\partial^2}{\partial \theta^2}. \tag{2.4}$$

Here u, v are the dimensionless fluid velocities in the r and θ directions and we have assumed the flow is independent of z and has no velocity component in the z-direction.

We set

$$x=r-R_1/d=(r^*-R_1)/d \tag{2.5}$$

and define the dimensionless gap width

$$\delta=d/R_1. \tag{2.6}$$

We see that

$$\frac{1}{r}=\frac{\delta}{1+\delta x} \tag{2.7}$$

so that all the terms in (2.1)–(2.4) involving $\partial/\partial\theta$ have a factor of order δ or δ^2 and are

thus relatively small if δ is small. We suppose that the outer fixed cylinder has equation

$$x = F(\theta) \tag{2.7a}$$

where $F(\theta)$ is an O(1) function. In terms of r^* the equation is

$$r^* = R_1 + dF(\theta), \qquad (F(0) = 1). \tag{2.8}$$

The aim is to let some of the nonlinear terms appear at the first approximation and this is achieved by setting

$$R\delta = \lambda \tag{2.9}$$

and considering $\delta \to 0$, $R \to \infty$ with λ fixed. This may be formalized by using a stream function $\psi(x, \theta)$ such that

$$u = \frac{-\delta}{1 + \delta x} \frac{\partial \psi}{\partial \theta}, \qquad v = \frac{\partial \psi}{\partial x}. \tag{2.10}$$

Consistent with this we may expand

$$u = \delta u_0(x, \theta) + \delta^2 u_1(x, \theta) + \ldots, \tag{2.11}$$

$$v = v_0(x, \theta) + \delta v_1(x, \theta) + \ldots, \tag{2.12}$$

$$p = p_0(x, \theta) + \delta p_1(x, \theta) + \ldots. \tag{2.13}$$

Upon substitution into the first momentum equation we find at lowest order in δ

$$\frac{\partial p_0}{\partial x} = 0 \tag{2.14}$$

and hence

$$p = p_0(\theta) + \delta p_1(x, \theta) + \ldots. \tag{2.15}$$

Then on using the second momentum equation we find, at lowest order,

$$u_0 \frac{\partial v_0}{\partial x} + v_0 \frac{\partial v_0}{\partial \theta} = -\frac{\mathrm{d}p_0}{\mathrm{d}\theta} + \frac{1}{\lambda} \frac{\partial^2 v_0}{\partial x^2}. \tag{2.16}$$

In terms of the stream function defined by (2.10), we have

$$\psi = \psi_0(x, \theta) + \delta \psi_1(x, \theta) + \ldots \tag{2.17}$$

and find

$$u_0 = -\partial \psi_0 / \partial \theta, \qquad v_0 = \partial \psi_0 / \partial x.$$

Hence (2.16) becomes

$$-\frac{\partial\psi_0}{\partial\theta}\frac{\partial^2\psi_0}{\partial x^2}+\frac{\partial\psi_0}{\partial x}\frac{\partial^2\psi_0}{\partial x\partial\theta}=-\frac{\mathrm{d}p_0}{\mathrm{d}\theta}+\frac{1}{\lambda}\frac{\partial^3\psi_0}{\partial x^3}. \tag{2.18}$$

It is convenient to introduce the cross-stream variable

$$\eta = x/F(\theta) \tag{2.19}$$

and we set

$$\psi_0 = G(\eta, \theta). \tag{2.20}$$

Then (2.18) becomes

$$G_{\eta\eta\eta}+\lambda F(\theta)\left(G_\theta G_{\eta\eta}-G_\eta G_{\theta\eta}\right)+\lambda F'(\theta)G_\eta^2-\lambda F^3(\theta)\frac{\mathrm{d}p_0}{\mathrm{d}\theta}=0. \tag{2.21}$$

The boundary and periodicity conditions are

$$\begin{aligned} &G_\eta = F(\theta), \quad G_\theta = 0 \quad \text{on} \quad \eta = 0;\\ &G_\eta = 0, \quad G_\theta = 0 \quad \text{on} \quad \eta = 1;\\ &G \text{ and } p_0 \text{ are periodic } (2\pi) \text{ in } \theta. \end{aligned} \tag{2.22}$$

The velocities to first order are

$$\delta u_0 = \delta\left(\eta\frac{F'(\theta)}{F(\theta)}G_\eta - G_\theta\right), \tag{2.23}$$

$$v_0 = \frac{1}{F(\theta)}G_\eta. \tag{2.24}$$

If we fix G at $\eta = 1$ to be equal to a constant K, then the condition $G_\theta = 0$ is satisfied. The system to be solved for the unknowns $G(x, \theta)$, $P(\theta)$ and K is then

$$G_{\eta\eta\eta}+\lambda F(\theta)\left(G_\theta G_{\eta\eta}-G_\eta G_{\theta\eta}\right)+\lambda\frac{\mathrm{d}F(\theta)}{\mathrm{d}\theta}G_\eta^2-F^3(\theta)\frac{\mathrm{d}P}{\mathrm{d}\theta}=0, \tag{2.25}$$

$$\begin{aligned} &G_\eta = F(\theta), \quad G = 0 \quad \text{on} \quad \eta = 0; \quad (a)\\ &G = K, \quad G_\eta = 0 \quad \text{on} \quad \eta = 1; \quad (b)\\ &G \text{ and } P \text{ are periodic } (2\pi) \text{ in } \theta. \quad (c) \end{aligned} \tag{2.26}$$

where $P = \lambda p_0$.

Given an initial profile $G(\eta, 0)$ and $P(0) = 0$ for a fixed K the system (2.25)–(2.26) may be marched forward in θ. This will not satisfy the periodicity conditions in general, and K must be adjusted together with the profile at $\theta = 0$ until these are satisfied. This is described further in Section 3.

3. Numerical scheme

A finite-difference scheme was used to obtain numerical solutions of the system (2.25)–(2.26). The equation (2.25) was integrated in the positive θ direction from $\theta = 0$ to $\theta = 2\pi$, and an iteration procedure used to ensure that the final solution obeyed the periodicity conditions (2.26c).

New variables, defined by

$$S = \frac{\partial G}{\partial \eta}, \qquad T = \frac{\partial S}{\partial \eta} \tag{3.1}$$

were used to reduce equation (2.25) to first-order form:

$$\frac{\partial T}{\partial \eta} + \lambda \left\{ F\left(T\frac{\partial G}{\partial \theta} - S\frac{\partial S}{\partial \theta} \right) + S^2 \frac{\mathrm{d}F}{\mathrm{d}\theta} \right\} - F^3 \frac{\mathrm{d}P}{\mathrm{d}\theta} = 0. \tag{3.2}$$

The boundary conditions (2.26a, b) are replaced by

$$G = 0, \quad S = F \quad \text{on} \quad \eta = 0; \tag{3.3}$$

$$G = K^{(n)}, \quad S = 0 \quad \text{on} \quad \eta = 1, \tag{3.4}$$

where K is assumed to have a known value, $K^{(n)}$, and n will be used (below) as the iteration index. At $\theta = 0$ we assume 'initial' conditions of the form

$$G = G_0^{(n)}(\eta), \quad S = S_0^{(n)}(\eta) = G_0^{(n)\prime}, \quad T = T_0^{(n)}(\eta) = G_0^{(n)\prime\prime}, \quad P = 0 \tag{3.5}$$

where $G_0^{(n)}(\eta)$ is a specified profile and the pressure is taken as zero at $\theta = 0$.

The system (3.1)–(3.5) was discretised onto a uniform mesh in η and θ, using central differences in each direction. At the current θ step there are $3N + 1$ unknowns P, $\{G_i, S_i, T_i\}$ $(i = 1, \ldots, N)$, where $i = 1$ and $i = N$ correspond to $\eta = 0$ and $\eta = 1$ respectively. These satisfy the $3N + 1$ equations given by the three discretised forms of (3.1), (3.2) ($3 \times (n - 1)$ equations) and the four boundary conditions (3.3), (3.4). The nonlinearity in (3.2) was removed by using a Newton iteration to convert the system into a linear matrix equation. The coefficient matrix contained a band of seven non-zero diagonals and a single column corresponding to the pressure term. Gaussian elimination was used to remove this column and the adjusted matrix was then solved using a standard routine for banded matrices.

Solutions for the velocity and pressure are thus obtained by computing forward from the initial profile (3.5) to $\theta = 2\pi$, where

$$G = G_1^{(n)}(\eta), \qquad S = S_1^{(n)}(\eta), \qquad T = T_1^{(n)}(\eta), \qquad P = P_1, \tag{3.6}$$

say. In general these profiles do not coincide with those in (3.5), violating the periodicity conditions. An iteration scheme was therefore devised in which the profiles (3.5) and (3.6) are equalised after several sweeps of the region $0 \leqslant \theta \leqslant 2\pi$. The scheme must account for variations in both the detailed shape of the velocity profile at $\theta = 0$ and the total volume flux, which depends on the (unknown) value of K. It appears that the latter is related to the periodicity of the pressure; an overall deficit in pressure from $\theta = 0$ to $\theta = 2\pi$ ($P_1 < 0$) allows the flow to be too fast and therefore corresponds to a value of K

too high, and an overall increase ($P_1 > 0$) corresponds to a value of K too low. After one sweep of the layer, the first part of the iteration procedure is therefore to adjust $K^{(n)}$ to a new value

$$K^{(n+1)} = K^{(n)} \pm \delta K^{(n)}, \qquad \text{according as} \qquad P_1 \gtrless 0. \tag{3.7}$$

After a few iterations with $\delta K^{(n)}$ held fixed, it was generally possible to obtain convergence by setting $\delta K^{(n)} = \frac{1}{2}\delta K^{(n-1)}$. An alternative method, also used successfully, was to base the new value of K on a linear interpolation of the two previous values of P_1.

The second stage is to adjust the detailed structure of the velocity profile, taking into account both the new shape given by (3.6) and the change in overall flux given by (3.7). Thus at the n(th) stage of the iteration we set

$$\begin{bmatrix} G_0^{(n+1)} \\ S_0^{(n+1)} \\ T_0^{(n+1)} \end{bmatrix} = \left\{ \bar{R} \begin{bmatrix} G_1^{(n)} \\ S_1^{(n)} \\ T_1^{(n)} \end{bmatrix} + (1 - \bar{R}) \begin{bmatrix} G_0^{(n)} \\ S_0^{(n)} \\ T_0^{(n)} \end{bmatrix} \right\} \frac{K^{(n+1)}}{K^{(n)}} \tag{3.8}$$

where $\bar{R}$ is a relaxation factor, which in most of the computations was taken as 0.5. Note that the formula for $S_0^{(n+1)}$ and the boundary condition, $S = F$ on $\eta = 0$, imply that in general there is a slight jump in the value of S on the first θ step along the inner cylinder wall. However, this did not affect convergence and the discontinuity is automatically smoothed out as $K^{(n+1)} \to K^{(n)}$ and convergence is completed.

The scheme was generally started from an initial approximation equivalent to the Couette-flow solution for constant gap width,

$$K^{(0)} = \tfrac{1}{2}, \qquad G_0^{(0)} = \eta - \tfrac{1}{2}\eta^2, \qquad S_0^{(0)} = 1 - \eta, \qquad T_0^{(0)} = -1. \tag{3.9}$$

For a typical run with $\lambda = 1$, $F = 1 + 0.1 \sin\theta$ and step-sizes of $\delta\eta = 0.1$, $\delta\theta = 2\pi/25$ it was found that after 9 iterations $|P_1| < 10^{-2}$, and $G_0^{(9)}$ and $G_1^{(9)}$ were identical to within a tolerance of 10^{-3}; at this stage the value of K had also converged to within a tolerance of less than 10^{-3}. A further 7 iterations improved the pressure tolerance to $|P_1| < 10^{-4}$ and the G_0 and K tolerances to less than 10^{-5}. About 3 or 4 Newton iterations were required to obtain convergence to within a tolerance of 10^{-7} on individual θ steps. Results were obtained for the profile

$$F = 1 + \alpha \sin\theta \qquad (0 \leqslant \alpha \leqslant 1) \tag{3.10}$$

for various values of λ and α, and are summarised in Table 1 and Figs. 2–7.

Some checks on the accuracy of the computations were performed using a finer mesh ($\delta\eta = 0.02$, $\delta\theta = 2\pi/100$) and for $\lambda = 1$, 20 and $\alpha = 0.1$, 0.5 these exhibited satisfactory agreement with the results obtained from the first two terms of a series expansion in powers of λ given in (4.1) below. For the coarser mesh the maximum percentage error appears to be about 3%. It was found that the forward integration in the θ direction remained stable, even through regions of quite severe reverse flow (see Figs. 5, 7) and the results obtained in such cases appear to be consistent with the behaviour suggested by asymptotic solutions of the equations described below. The upstream influence associated with reverse flow does not invalidate the method of solution since upstream influence can

Table 1
Value of the flux constant K, using step-sizes $\delta\eta = 1/10$, $\delta\theta = 2\pi/25$ (theoretical values are given for $\lambda = 0$, $\alpha = 0$ and $\alpha = 1$)

	λ				
α	0	1	20	40	100
0	$\frac{1}{2}$	$\frac{1}{2}$	$\frac{1}{2}$	$\frac{1}{2}$	$\frac{1}{2}$
0.1	0.4925	0.4927	0.4925	0.4921	0.4903
0.5	$\frac{1}{3}$	0.3357	0.3352	0.3337	0.3244
0.8	0.1371	0.1407	–	–	–
1	0	0	0	0	0

occur in the numerical scheme through the iteration procedure. Thus, provided the forward integration remains stable, the final solution should not be discounted on these grounds.

The major features of the solution can be observed in Figs. 2–7. For an outer-wall variation of the form (3.10) there is a region of compression near $\theta = 3\pi/2$ where the pressure falls and the flow attains a maximum forward velocity (Fig. 5). Around $\theta = \pi/2$ there is a region of expansion associated with a pressure rise and often separation and large regions of reverse flow. The total volume flux, represented by the value of K in Table 1, appears to be dependent to a large extent on the maximum width restriction imposed by the cylinders (which is fixed by the value of α in (3.10)) and is relatively insensitive to the value of λ. In the next sections we derive various asymptotic solutions of the system

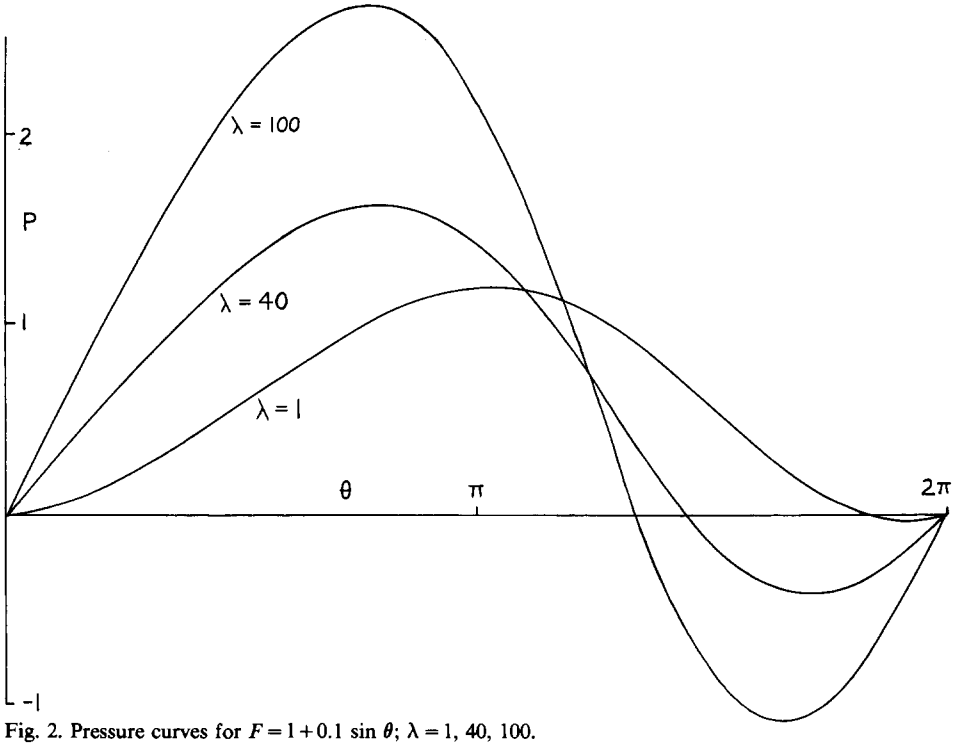

Fig. 2. Pressure curves for $F = 1 + 0.1 \sin\theta$; $\lambda = 1$, 40, 100.

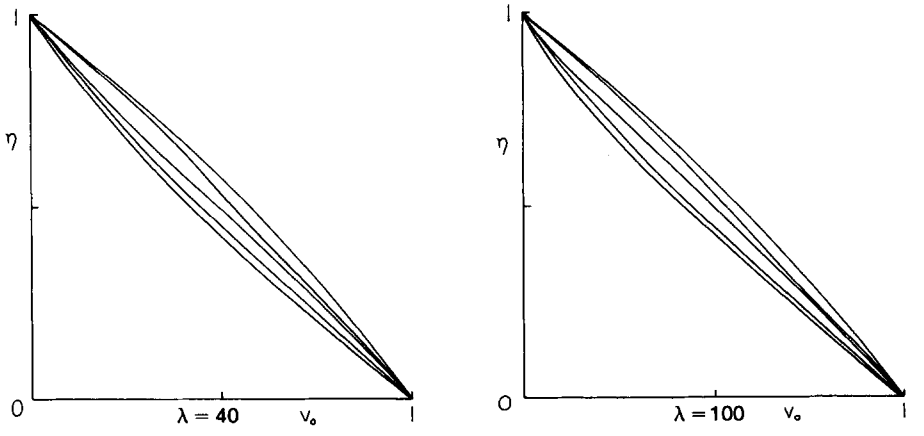

Fig. 3. Velocity profiles for $F = 1 + 0.1 \sin \theta$ at (left to right) $\theta/2\pi = \frac{1}{5}, \frac{2}{5}, 0, \frac{3}{5}, \frac{4}{5}$.

(2.25)–(2.26) which confirm this, and also allow a more detailed interpretation of the behaviour of the numerical solutions.

4. Linear theory

As the parameter λ tends to zero the solution of the system (2.25)–(2.26) can be expanded

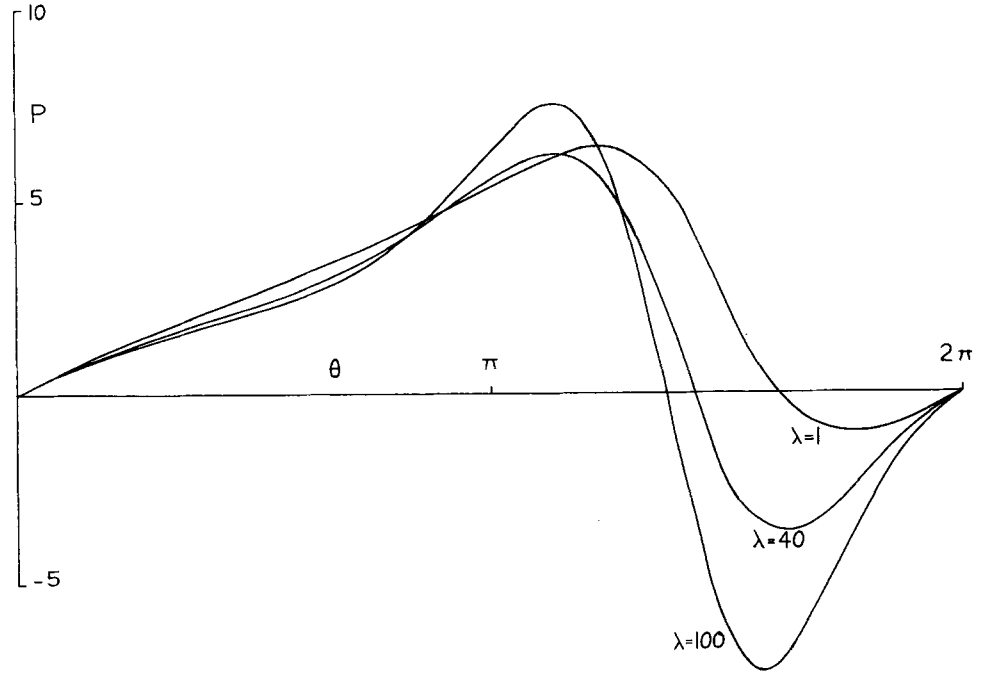

Fig. 4. Pressure curves for $F = 1 + 0.5 \sin \theta$; $\lambda = 1, 40, 100$.

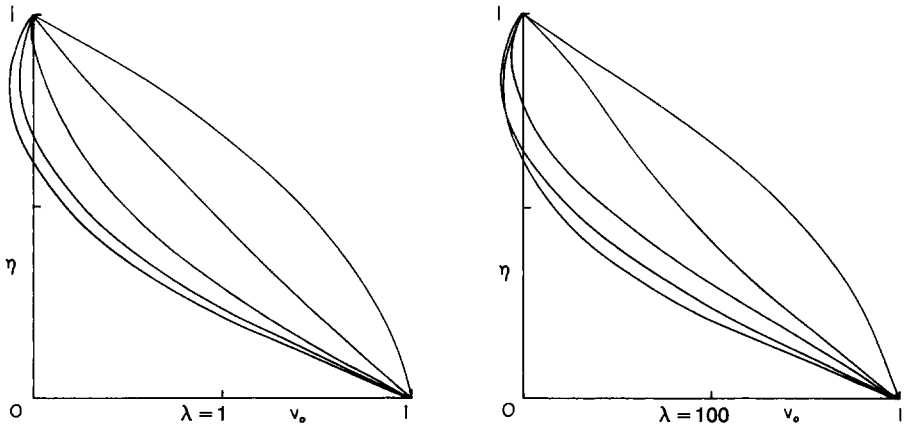

Fig. 5. Velocity profiles for $F = 1 + 0.5 \sin\theta$ at (left to right) $\theta/2\pi = \frac{1}{5}, \frac{2}{5}, 0, \frac{3}{5}, \frac{4}{5}$.

in the form

$$G(\eta, \theta) = G_0 + \lambda G_1 + \ldots,$$

$$P(\theta) = P_0 + \lambda P_1 + \ldots, \tag{4.1}$$

$$K = K_0 + \lambda K_1 + \ldots, (\lambda \to 0),$$

where the leading-order terms satisfy the linear equation

$$\frac{\partial^3 G_0}{\partial \eta^3} = F^3 \frac{\mathrm{d}P_0}{\mathrm{d}\theta} \tag{4.2}$$

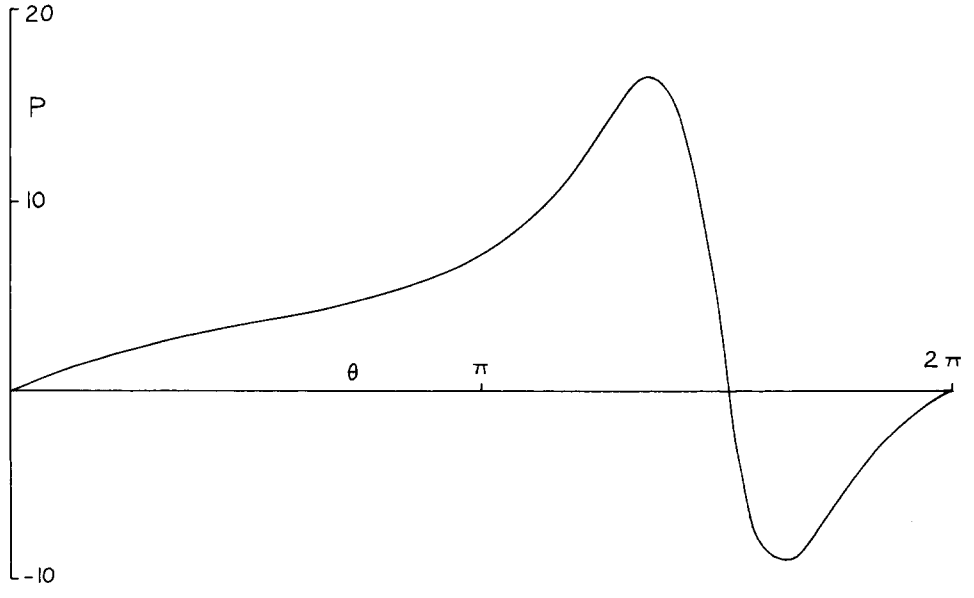

Fig. 6. Pressure curve for $F = 1 + 0.8 \sin\theta$; $\lambda = 1$.

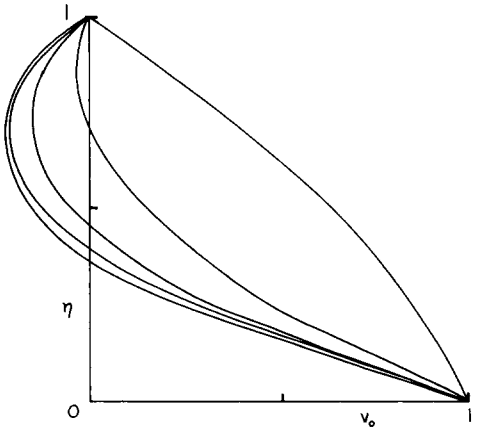

Fig. 7. Velocity profiles for $F = 1 + 0.8 \sin\theta$, $\lambda = 1$ and at (left to right) $\theta/2\pi = \frac{1}{5}, \frac{2}{5}, 0, \frac{3}{5}, \frac{4}{5}$.

with boundary conditions

$$\begin{aligned} &G_0 = 0, \quad \frac{\partial G_0}{\partial \eta} = F \quad \text{on} \quad \eta = 0; \\ &G_0 = K_0, \quad \frac{\partial G_0}{\partial \eta} = 0 \quad \text{on} \quad \eta = 1. \end{aligned} \tag{4.3}$$

In addition, both P_0 and G_0 must be periodic. Since $\partial^4 G_0/\partial\eta^4 = 0$ the general solution of (4.2) has the form

$$G_0 = \sum_{n=0}^{3} a_n(\theta)\eta^n. \tag{4.4}$$

The four conditions (4.3) are satisfied by taking

$$a_0 = 0, \quad a_1 = F, \quad a_2 = 3K_0 - 2F, \quad a_3 = F - 2K_0 \tag{4.5}$$

and, from (5.2), we obtain the pressure as

$$P_0 = \int_0^\theta \frac{F - 2K_0}{F^3}\,\mathrm{d}\theta. \tag{4.6}$$

The periodicity of F ensures that G_0 is periodic, but from (4.6) we see that K_0 must be chosen to have the value

$$K_0 = \tfrac{1}{2}\int_0^{2\pi} F^{-2}\mathrm{d}\theta \Big/ \int_0^{2\pi} F^{-3}\mathrm{d}\theta \tag{4.7}$$

in order that P_0 is periodic. It follows from (4.7) that the volume flux, K_0, satisfies the constraints

$$\tfrac{1}{2}\min(F) < K_0 < \tfrac{1}{2}\max(F), \tag{4.8}$$

with $K_0 = \frac{1}{2}$ if $F = 1$.

For the profile (3.10) we obtain, from (4.7),

$$K_0 = \frac{\frac{1}{2}(1-\alpha^2)}{\left(1+\frac{1}{2}\alpha^2\right)} \qquad (0 \leqslant \alpha \leqslant 1) \tag{4.9}$$

and the velocity profile is given by

$$v = \frac{1}{F}\frac{\partial G_0}{\partial \eta} = 1 + 2\left(\frac{3K_0}{F} - 2\right)\eta + 3\left(1 - \frac{2K_0}{F}\right)\eta^2. \tag{4.10}$$

Separation occurs at the outer wall when $\partial^2 G_0/\partial\eta^2(1, \theta) = 0$. From (4.10) this requires $K_0 = \frac{1}{3}F$, or

$$\tfrac{1}{3}(1 + \alpha \sin\theta) = \tfrac{1}{2}\frac{(1-\alpha^2)}{\left(1+\frac{1}{2}\alpha^2\right)}. \tag{4.11}$$

Thus, as the variation in gap width, α, increases from zero, separation first occurs on the outer wall at the point of maximum width $\theta = \pi/2$, when

$$\alpha = \tfrac{1}{2}(\sqrt{13} - 3) = 0.303. \tag{4.12}$$

As the value of α increases beyond 0.303, the region of reverse flow becomes more extensive, with the points of separation and reattachment placed symmetrically about $\theta = \pi/2$. Eventually, as $\alpha \to 1$, the two points meet at $\theta = 3\pi/2$ and reverse flow occurs for all $\theta \neq 3\pi/2$. This is to be expected, since the two cylinders now touch at $\theta = 3\pi/2$ and no fluid can pass between them. Thus $K_0 = 0$ and, from (4.10), the velocity profile has the form

$$v = 1 - 4\eta + 3\eta^2, \qquad (0 < \eta < 1), \tag{4.13}$$

exhibiting reverse flow for $\frac{1}{3} < \eta < 1$, and forward flow for $0 < \eta < \frac{1}{3}$ driven by the rotation of the inner cylinder.

The solution for G_1 in (4.1) can be shown to have the form

$$G_1 = \sum_{n=2}^{7} \beta_n(\theta)\eta^n \tag{4.14}$$

and detailed work shows that G_1 has a factor $F'(\theta)$. It can also be shown that $K_1 = 0$.

We can confirm that our theory for small λ reproduces the results of DiPrima and Stuart [7] who consider slightly eccentric cylinders equivalent to

$$\alpha = O(\delta^{1/2}) \tag{4.15}$$

in (3.10). In addition

$$R = O(\delta^{-1/2}) \tag{4.16}$$

in order to conform with DiPrima and Stuart's case of fixed Taylor number. Then

$$\lambda = R\delta = O(\delta^{1/2}) \tag{4.17}$$

and the stream function (for the complete Navier-Stokes equations) is

$$\psi = G_0(\eta) + O(\delta), \tag{4.18}$$

allowing for the factor of $\delta^{1/2}$ (from $F'(\theta)$) in G_1. From (4.9)

$$K_0 = \tfrac{1}{2} + O(\alpha^2) \tag{4.19}$$

and the velocity v in the θ-direction is $G_{0\eta}/F(\theta) + O(\delta)$ which reduces to

$$v = (1-\eta) + \alpha \sin\theta(3\eta^2 - 3\eta) + O(\delta). \tag{4.20}$$

DiPrima and Stuart's co-ordinates ϕ and x may be shown to be related to our θ and η by

$$x + \tfrac{1}{2} = \eta + O(\delta),$$

$$\phi = \theta - \frac{\pi}{2} + O(\delta), \tag{4.21}$$

so that (4.20) reduces to

$$v = (\tfrac{1}{2} - x) + \alpha \cos\phi\left(3\left(x^2 - \tfrac{1}{4}\right)\right) + O(\delta) \tag{4.22}$$

which, allowing for the different non-dimensionalisation, reduces to DiPrima and Stuart's [7]

$$V_0 + \varepsilon V_1 \tag{4.23}$$

for the azimuthal velocity provided $\varepsilon = \alpha$, where ε is their eccentricity ratio. A geometric consideration of the meaning of (3.10) shows that it is the expansion to $O(\delta^{3/2})$ of the gap width when the outer cylinder is a circular cylinder with its centre at distance $\alpha\delta$ (in units of R_1) from the origin. Thus $\alpha = \varepsilon$.

Summarising, if the local gap width $d_L(\theta)$ is

$$d_L(\theta) = R_1\delta(1 + \alpha\sin\theta + \ldots), \qquad \alpha = O(\delta^{1/2}), \tag{4.24}$$

then our flow, expanded for fixed Taylor number and thus $R = O(\delta^{-1/2})$, gives the first two terms of DiPrima and Stuart's series for the eccentric cylinders case with $\varepsilon = O(\delta^{1/2})$.

When $R = O(\delta^{-1})$, of course, these two terms are included in our first approximation.

5. Nearly touching cylinders, $\alpha \to 1$

The analysis of the situation in which the cylinders nearly touch can be extended to general values of the parameter λ. Let $\varepsilon(\ll 1)$ denote the minimum non-dimensional width between the two cylinders and suppose that this occurs at $\theta = \theta_0$. Locally we may

then assume that F has the form

$$F(\theta) \sim \varepsilon + a(\theta - \theta_0)^2 + \ldots \qquad (\theta \to \theta_0 \pm) \tag{5.1}$$

where a is a known constant. Variations in the solution occur in the region near θ_0 where

$$\theta' = \varepsilon^{-1/2}(\theta - \theta_0) = O(1). \tag{5.2}$$

Here

$$F = \varepsilon(1 + a\theta'^2) + O(\varepsilon^2), \qquad (\varepsilon \to 0). \tag{5.3}$$

The system (2.25), (2.26) suggests that locally the solution can be expanded in the form

$$\begin{aligned} G &= \varepsilon \bar{G}_0(\eta, \theta') + \ldots, \\ P &= \varepsilon^{-3/2}\bar{P}_0(\theta') + \ldots, \qquad (\varepsilon \to 0), \end{aligned} \tag{5.4}$$

and that the expansion for the flux constant K begins

$$K = \varepsilon \bar{K}_0 + \ldots, \tag{5.5}$$

consistent with the requirement that $K = 0$ when the gap between the cylinders is completely closed ($\varepsilon = 0$).

At order ε, substitution of (5.4), (5.5) into (2.25)–(2.26) yields the system

$$\begin{aligned} &\frac{\partial^3 \bar{G}_0}{\partial \eta^3} = (1 + a\theta'^2)^3 \frac{d\bar{P}_0}{d\theta'}, \\ &\frac{\partial \bar{G}_0}{\partial \eta} = 1 + a\theta'^2, \quad \bar{G}_0 = 0 \quad \text{on} \quad \eta = 0, \\ &\frac{\partial \bar{G}_0}{\partial \eta} = 0, \qquad\quad \bar{G}_0 = \bar{K}_0 \quad \text{on} \quad \eta = 1, \end{aligned} \tag{5.6}$$

similar in form to (4.2), (4.3) above. We now obtain

$$\bar{G}_0 = (1 - 2\bar{K}_0 + a\theta'^2)\eta^3 + (3K_0 - 2 - 2a\theta'^2)\eta^2 + (1 + a\theta'^2)\eta, \tag{5.7}$$

and

$$\bar{P}_0 = 6\int_{-\infty}^{\theta'} \frac{(1 - 2\bar{K}_0 + a\theta'^2)d\theta'}{(1 + a\theta'^2)^3} \tag{5.8}$$

where $\bar{K}_0$ is still to be determined. We can expect that its determination requires the application of the periodicity condition (2.26c) but this, in turn, requires a discussion of the outer flow where $\theta \neq \theta_0$. Clearly an analytic solution of the full equations for general values of λ is not possible in this region, although (4.13) gives an approximation to the

form that it takes for arbitrary $F(\theta)$ if $\lambda \ll 1$. Fortunately we may find $\bar{K}_0$ without reference to the detailed structure of the solution, since it is clear that $G = O(1)$ and $P = O(1)$ in the outer flow. Since $P = O(\varepsilon^{-3/2})$ in the region near θ_0, it follows that $\bar{K}_0$ must be chosen in (5.8) to ensure that $\bar{P}_0 \to 0$ as $\theta' \to \infty$. Thus

$$\bar{K}_0 = \tfrac{2}{3}, \tag{5.9}$$

$$\bar{P}_0 = \frac{-2\theta'}{(1 + a\theta'^2)^2}, \qquad (-\infty < \theta' < \infty), \tag{5.10}$$

and

$$\bar{G}_0 = \left(a\theta'^2 - \tfrac{1}{3}\right)\eta^3 - 2a\theta'^2\eta^2 + (1 + a\theta'^2)\eta, \qquad (-\infty < \theta' < \infty). \tag{5.11}$$

The solutions (5.10) and (5.11) show that near θ_0 the pressure first rises to a maximum at $\theta' = -(3a)^{-1/2}$, reattachment having occurred in the adverse pressure gradient at $\theta' = -a^{-1/2}$. For $-(3a)^{-1/2} < \theta' < (3a)^{-1/2}$ the pressure gradient is favourable and at $\theta' = 0$ the flow in the gap is fully forward, with $\partial \bar{G}_0/\partial\eta = 1 - \eta^2$. Beyond $\theta' = (3a)^{-1/2}$ the pressure gradient is again adverse and separation occurs on the outer cylinder wall at $\theta' = a^{-1/2}$. These features of the solution are consistent with the behaviour of the numerical solution shown in Figs. 6 and 7. There, $\alpha = 0.8$ so that

$$\varepsilon = 1 - \alpha = 0.2 \tag{5.12}$$

The maximum constriction occurs at $\theta_0 = 3\pi/2$ where $F(\theta)$, given by (3.10), may be written in the form

$$F = \varepsilon(1 + a\theta'^2) + \varepsilon^2(b\theta'^4 + c\theta'^2) + O(\varepsilon^3), \qquad (\varepsilon \to 0), \qquad (\theta' = O(1)), \tag{5.13}$$

with

$$a = \tfrac{1}{2}, \qquad b = -\tfrac{1}{24}, \qquad c = -\tfrac{1}{2}. \tag{5.14}$$

The above theory may easily be extended to take into account the correction term of $O(\varepsilon^2)$ in (5.13). We set

$$\left.\begin{aligned} G &= \varepsilon\bar{G}_0 + \varepsilon^2\bar{G}_1 + \varepsilon^{5/2}\bar{G}_2 + \ldots \\ P &= \varepsilon^{-3/2}\bar{P}_0 + \varepsilon^{-1/2}\bar{P}_1 + \bar{P}_2 + \ldots \end{aligned}\right\}, \qquad (\theta' = O(1)), \tag{5.15}$$

and the equations for $\bar{P}_1$, $\bar{G}_1$ are again linear. The periodicity requirement that $\bar{P}_1 \to 0$, $(\theta' \to \pm\infty)$, leads to the expansion

$$K = \tfrac{2}{3}\varepsilon - \tfrac{2}{3}ba^{-2}\varepsilon^2 + O(\varepsilon^{5/2}) \tag{5.16}$$

for the flux constant.

The next terms $\bar{G}_2$, $\bar{P}_2$ and the $O(\varepsilon^{5/2})$ correction to K involve the parameter λ, and the matching conditions for $\bar{P}_2$ as $\theta' \to \pm\infty$ require an evaluation of the pressure in the outer

flow. An explicit evaluation can be made in the limit $\lambda \to 0$, since then we have

$$P(\theta) \simeq 6\int_0^{\theta} F_0^{-2}\mathrm{d}\theta \qquad (0 \leqslant \theta < \theta_0) \tag{5.17}$$

and

$$P(\theta) \simeq -6\int_{\theta}^{2\pi} F_0^{-2}\mathrm{d}\theta \qquad (\theta_0 < \theta \leqslant 2\pi) \tag{5.18}$$

where it is assumed that $P(0) = P(2\pi)$ in order to satisfy the periodicity condition. For the profile (3.10) in which $\alpha = 1 - \varepsilon$, F_0 is given by

$$F_0 = 1 + \sin\theta$$

so that

$$F_0 \sim a(\theta - \theta_0)^2 + b(\theta - \theta_0)^4 + \ldots \quad (\theta \to \theta_0 \pm), \tag{5.19}$$

where a and b are given by (5.14). It then follows from (5.17) and (5.18) that

$$P \sim -\frac{2}{a^2(\theta - \theta_0)^3} + \frac{12b}{a^3(\theta - \theta_0)} + 4, \qquad (\theta \to \theta_0 \pm). \tag{5.20}$$

The two leading terms match with the solutions in the inner region for $\bar{P}_0$ and $\bar{P}_1$ respectively and the finite part of the expression (5.20) indicates that

$$\bar{P}_2 \to 4, \qquad (\theta' \to \pm\infty). \tag{5.21}$$

This can be expected to fix the $O(\varepsilon^{5/2})$ correction to the value of K in (5.16); for $\lambda = 0$ the correction is actually zero and $\bar{P}_2 = 4$. The result (5.21) means that in the neighbourhood of $\theta_0 = 3\pi/2$ we can expect that, provided the value of λ does not have a significant effect, the pressure curve given to leading order by (5.10) will be displaced upwards by an amount 4 and this is consistent with the behaviour found in the numerical solution for $\lambda = 1$, $\varepsilon = 0.2$ (Fig. 6). The pressure maxima and minima based on (5.10) are then

$$\pm\varepsilon^{-3/2}\frac{9}{8\sqrt{3a}} \simeq \pm 10.3 \tag{5.22}$$

and occur at

$$\theta = \theta_0 \mp \varepsilon^{1/2}\left(\frac{1}{3a}\right)^{1/2} \simeq \frac{3\pi}{2} \mp 0.37. \tag{5.23}$$

These values are in good agreement with Fig. 6, and the value $K = 0.1377$ obtained from (5.16) compares well with the numerical value of 0.1407.

It should be noted that the leading two terms in (5.15) and (5.16) are valid for any finite λ and demonstrate how the region of maximum constriction controls the volume flux in this case, independent of the outer flow which cannot, in general, be found

analytically. Since $\bar{P}_2$ and $\bar{G}_2$ are proportional to λ, it seems likely that the inner expansions (5.15), (5.16) will eventually fail when $\lambda = O(\varepsilon^{-3/2})$.

6. Nearly constant gap width, $F \simeq 1$

As the gap width between the cylinders approaches a constant value, the flow must tend to the classical Couette solution. This simplification allows some insight into the solution of the nonlinear system (2.25), (2.26) for $\lambda \gg 1$.

We assume that the outer cylinder wall is given by

$$F(\theta) = 1 + \alpha f(\theta) \tag{6.1}$$

where $\alpha \ll 1$ and f is an arbitrary periodic function of θ. The solutions for G and P may then be expanded in powers of α:

$$G = \tilde{G}_0(\eta, \theta) + \alpha\tilde{G}_1(\eta, \theta) + \alpha^2\tilde{G}_2(\eta, \theta) + \ldots, \qquad (\alpha \to 0), \tag{6.2}$$

$$P = \tilde{P}_0(\theta) + \alpha\tilde{P}_1(\theta) + \alpha^2\tilde{P}_2(\theta) + \ldots, \qquad (\alpha \to 0), \tag{6.3}$$

and the flux constant K has the form

$$K = \tilde{K}_0 + \alpha\tilde{K}_1 + \alpha^2\tilde{K}_2 + \ldots, \qquad (\alpha \to 0). \tag{6.4}$$

Substitution of (6.1)–(6.4) into the full system (2.25), (2.26) leads to a succession of problems for $\tilde{G}_i$, $\tilde{P}_i$ and $\tilde{K}_i$ $(i = 0, 1, \ldots)$.

At leading order we obtain

$$\frac{\partial^3\tilde{G}_0}{\partial\eta^3} = -\lambda\left(\frac{\partial\tilde{G}_0}{\partial\theta}\frac{\partial^2\tilde{G}_0}{\partial\eta^2} - \frac{\partial\tilde{G}_0}{\partial\eta}\frac{\partial^2\tilde{G}_0}{\partial\eta\partial\theta}\right) + \frac{\mathrm{d}\tilde{P}_0}{\mathrm{d}\theta} \tag{6.5}$$

with boundary conditions

$$\tilde{G}_0 = 0, \qquad \frac{\partial\tilde{G}_0}{\partial\eta} = 1 \qquad \text{on} \qquad \eta = 0,$$

$$\tilde{G}_0 = \tilde{K}_0, \qquad \frac{\partial\tilde{G}_0}{\partial\eta} = 0 \qquad \text{on} \qquad \eta = 1. \tag{6.6}$$

These conditions suggest that the solution for $\tilde{G}_0$ is independent of θ. This implies that $\tilde{P}_0$ is linear in θ, but since it must also be periodic, we must have

$$\tilde{P}_0 = 0. \tag{6.7}$$

From (6.5) and (6.6) we then obtain the Couette 'narrow-gap' solution

$$\tilde{G}_0 = \eta - \tfrac{1}{2}\eta^2, \qquad \tilde{K}_0 = \tfrac{1}{2}. \tag{6.8}$$

At order α, $\tilde{G}_1$, $\tilde{P}_1$ and $\tilde{K}_1$ are found to satisfy the equation

$$\frac{\partial^3 \tilde{G}_1}{\partial \eta^3} = \lambda\left\{\frac{\partial \tilde{G}_1}{\partial \theta} + (1-\eta)\frac{\partial^2 \tilde{G}_1}{\partial \eta \partial \theta} - f'(1-\eta)^2\right\} + \frac{\mathrm{d}\tilde{P}_1}{\mathrm{d}\theta} \tag{6.9}$$

and boundary conditions

$$\begin{aligned} &\tilde{G}_1 = 0, \quad \frac{\partial \tilde{G}_1}{\partial \eta} = f \quad \text{on} \quad \eta = 0, \\ &\tilde{G}_1 = \tilde{K}_1, \quad \frac{\partial \tilde{G}_1}{\partial \eta} = 0 \quad \text{on} \quad \eta = 1. \end{aligned} \tag{6.10}$$

In order to proceed with the solution we assume that $f(\theta)$ can, without loss of generality, be represented by the Fourier series

$$f(\theta) = f_0 + \sum_{n=1}^{\infty} f_n \mathrm{e}^{in\theta} + f_n^* \mathrm{e}^{-in\theta} \tag{6.11}$$

where * denotes complex conjugate. Corresponding periodic forms for $\tilde{G}_1$ and $\tilde{P}_1$ are

$$\tilde{G}_1 = g_0(\eta) + \sum_{n=1}^{\infty} g_n(\eta)\mathrm{e}^{in\theta} + g_n^*(\eta)\mathrm{e}^{-in\theta}, \tag{6.12}$$

$$\tilde{P}_1 = \tilde{p}_0 + \sum_{n=1}^{\infty} \tilde{p}_n \mathrm{e}^{in\theta} + \tilde{p}_n^* \mathrm{e}^{-in\theta}. \tag{6.13}$$

The leading coefficients in the series, f_0, g_0 and $\tilde{p}_0$ are all real. Substitution into (6.9), (6.10) yields

$$g_0''' = 0; \qquad g_0(0) = 0, \qquad g_0'(0) = f_0, \qquad g_0(1) = \tilde{K}_1, \qquad g_0'(1) = 0 \tag{6.14}$$

and

$$\begin{aligned} &g_n''' = \lambda in\left\{g_n + (1-\eta)g_n' - (1-\eta)^2 f_n\right\} + in\tilde{p}_n; \\ &g_n(0) = 0, \qquad g_n'(0) = f_n, \qquad g_n(1) = 0, \qquad g_n'(1) = 0. \end{aligned} \qquad (n \geqslant 1) \tag{6.15}$$

The $n = 0$ system is easily solved to give

$$g_0 = f_0\left(\eta - \tfrac{1}{2}\eta^2\right), \qquad \tilde{K}_1 = \tfrac{1}{2}f_0. \tag{6.16}$$

For $n \geqslant 1$ it is convenient to write

$$g_n = h_n(\eta) - f_n(1-\eta)^2 \tag{6.17}$$

so that h_n satisfies

$$h_n''' - in\lambda\left(h_n + (1-\eta)h_n'\right) = in\tilde{p}_n, \tag{6.18}$$

$$h_n(0) = f_n, \qquad h_n'(0) = -f_n, \qquad h_n(1) = 0, \qquad h_n'(1) = 0. \tag{6.19}$$

Although the full solution can be expressed in terms of Airy functions, the main interest is in the form of the solution for large Reynolds numbers, $\lambda \to \infty$. The system (6.18), (6.19) can then be solved by boundary-layer techniques, and the domain $0 \leqslant \eta \leqslant 1$ must be divided into three regions, a core where $\eta = O(1)$, a boundary layer on the inner cylinder, where

$$\eta_2 = \lambda^{1/2}\eta = O(1), \tag{6.20}$$

and a boundary layer on the outer cylinder, where

$$\eta_1 = \lambda^{1/3}(1-\eta) = O(1). \tag{6.21}$$

These scalings and (6.18) and (6.19) suggest expansions of the form

$$\tilde{p}_n = \lambda \bar{p}_0 + \lambda^{2/3}\bar{p}_1 + \ldots \tag{6.22}$$

and

$$h_n = \bar{h}_0(\eta) + \lambda^{-1/3}\bar{h}_1 + \ldots \qquad \text{(core)}, \tag{6.23}$$

$$h_n = \tilde{h}_0(\eta_2) + \lambda^{-1/3}\tilde{h}_1(\eta_2) + O(\lambda^{-1/2}) \qquad \text{(inner boundary layer)}, \tag{6.24}$$

$$h_n = \lambda^{-1/3}\hat{h}_1(\eta_1) + \ldots \qquad \text{(outer boundary layer)}. \tag{6.25}$$

In the core, the equations for $\bar{h}_i$, $\bar{p}_i$ are

$$\bar{h}_i + (1-\eta)\bar{h}_i' = -\bar{p}_i \qquad (i = 0, 1) \tag{6.26}$$

and so

$$\bar{h}_i = \bar{a}_i(1-\eta) - \bar{p}_i \qquad (i = 0, 1) \tag{6.27}$$

where $\bar{a}_i$, $(i = 0, 1)$, are arbitrary constants.

In the inner boundary layer, $\tilde{h}_0$ satisfies the equation

$$\tilde{h}_0''' - in\tilde{h}_0' = 0 \tag{6.28}$$

and boundary conditions

$$\tilde{h}_0(0) = f_n, \qquad \tilde{h}_0'(0) = 0, \tag{6.29}$$

and since the solution must not grow exponentially into the core,

$$\tilde{h}_0 = f_n. \tag{6.30}$$

A similar consideration of the equation for $\tilde{h}_1$ gives

$$\tilde{h}_1 = 0. \tag{6.31}$$

Matching with the core solution (6.23) now gives the conditions

$$\bar{h}_0 = f_n, \bar{h}_1 = 0 \qquad \text{at} \quad \eta = 0, \tag{6.32}$$

so that

$$\bar{a}_0 = f_n + \bar{p}_0, \qquad \bar{a}_1 = \bar{p}_1. \tag{6.33}$$

Thus, as $\eta \to 1$,

$$\bar{h}_0 \to -\bar{p}_0, \qquad \bar{h}_1 \to -\bar{p}_1. \tag{6.34}$$

As might be expected, a consistent solution in the boundary layer on the outer wall is only possible if the core solution itself obeys the normal velocity condition $h_n(1) = 0$ at leading order. It then follows from (6.34) that

$$\bar{p}_0 = 0. \tag{6.35}$$

The boundary-layer function $\hat{h}_1$ is then generated by $\bar{a}_0 = f_n$ in (6.27).

Substitution of (6.25) into (6.18) yields the equation

$$\hat{h}_1''' + in\left(\hat{h}_1 - \eta_1 \hat{h}_1'\right) = -in\bar{p}_1. \tag{6.36}$$

From (6.19) the conditions at the cylinder wall are

$$\hat{h}_1(0) = 0, \qquad \hat{h}_1'(0) = 0 \tag{6.37}$$

and, from matching with the core solution $\bar{h}_0$, we also require

$$\hat{h}_1 \sim f_n \eta_1, \qquad (\eta_1 \to \infty). \tag{6.38}$$

The solution of (6.36)–(6.38) can be obtained by first differentiating (6.36) to give a form of Airy's equation. The required solution satisfying (6.37) and (6.38) is

$$\hat{h}_1 = 3 f_n n^{-1/3} \, \mathrm{e}^{-i\pi/6} \int_0^z \left\{ \int_0^z \mathrm{Ai}(z_1) \mathrm{d}z_1 \right\} \mathrm{d}z \tag{6.39}$$

where

$$z = \mathrm{e}^{i\pi/6} n^{1/3} \eta_1. \tag{6.40}$$

The original third-order equation (6.36) then fixes the value of $\bar{p}_1$ as

$$\bar{p}_1 = 3 f_n n^{-1/3} \mathrm{e}^{-i\pi/6} |\mathrm{Ai}'(0)|, \qquad (\mathrm{Ai}'(0) = -0.2582\ldots), \tag{6.41}$$

showing that the pressure distribution between the cylinders is now controlled mainly by the dynamics of the boundary-layer flow on the outer cylinder wall.

We may also note that the system (6.18)–(6.19) has simple solutions in the limit $\lambda \to 0$.

In this case

$$\begin{aligned} \tilde{p}_n &= -\frac{6i}{n} f_n + \mathrm{O}(\lambda), \\ g_n &= f_n \eta (1-\eta)^2 + \mathrm{O}(\lambda) \end{aligned} \qquad (\lambda \to 0), \qquad (n \geqslant 1). \tag{6.42}$$

The first correction to the flux constant, K, arises from the $\mathrm{O}(\alpha^2)$ terms in the basic expansions (6.2)–(6.4). These satisfy the equation

$$\frac{\partial^3 \tilde{G}_2}{\partial \eta^3} = \lambda \left\{ \frac{\partial \tilde{G}_2}{\partial \theta} + (1-\eta) \frac{\partial^2 \tilde{G}_2}{\partial \eta \partial \theta} + \frac{\partial \tilde{G}_1}{\partial \eta} \frac{\partial^2 \tilde{G}_1}{\partial \eta \partial \theta} - \frac{\partial \tilde{G}_1}{\partial \theta} \frac{\partial^2 \tilde{G}_1}{\partial \eta^2} \right\}$$

$$+\lambda f \left\{ \frac{\partial \tilde{G}_1}{\partial \theta} + (1-\eta) \frac{\partial^2 \tilde{G}_1}{\partial \eta \partial \theta} \right\} - 2\lambda f'(1-\eta) \frac{\partial \tilde{G}_1}{\partial \eta} + 3f \frac{\mathrm{d}\tilde{P}_1}{\mathrm{d}\theta} + \frac{\mathrm{d}\tilde{P}_2}{\mathrm{d}\theta}, \tag{6.43}$$

and boundary conditions

$$\begin{aligned} &\tilde{G}_2 = 0, \qquad \frac{\partial \tilde{G}_2}{\partial \eta} = 0 \qquad (\eta = 0); \\ &\tilde{G}_2 = \tilde{K}_2, \qquad \frac{\partial \tilde{G}_2}{\partial \eta} = 0 \qquad (\eta = 1), \end{aligned} \tag{6.44}$$

with, in addition, the usual periodicity requirements on $\tilde{G}_2$ and $\tilde{P}_2$.

Some progress can be made by restricting attention to the wall profile (3.10) in which case

$$f(\theta) = \sin\theta, \qquad f_1 = -\frac{i}{2}, \qquad f_n = 0 \qquad (n \neq 1) \tag{6.45}$$

and, from the preceding analysis,

$$\begin{aligned} \tilde{G}_1 &= g_1 \, \mathrm{e}^{i\theta} + g_1^* \, \mathrm{e}^{-i\theta} + g_0, \\ \tilde{P}_1 &= \tilde{p}_1 \, \mathrm{e}^{i\theta} + \tilde{p}_1^* \, \mathrm{e}^{-i\theta} + \tilde{p}_0. \end{aligned} \tag{6.46}$$

The solution for $\tilde{G}_2$ can be written in the form

$$\tilde{G}_2 = \tilde{g}_0(\eta) + \sum_{n=1}^{\infty} \tilde{g}_n(\eta) \, \mathrm{e}^{in\theta} + \tilde{g}_n^* \, \mathrm{e}^{-in\theta} \tag{6.47}$$

and consideration of terms independent of θ in (6.43)–(6.44) yields

$$\tilde{g}_0''' = -\lambda \{ i(g_1 g_1^{*\prime\prime} - g_1^* g_1'') + \tfrac{1}{2}(g_1 + g_1^*) + \tfrac{3}{2}(1-\eta)(g_1' + g_1^{*\prime}) - \tfrac{3}{2}(\tilde{p}_1 + \tilde{p}_1^*), \tag{6.48}$$

where

$$\tilde{g}_0(0)=0, \qquad \tilde{g}_0'(0)=0, \qquad \tilde{g}_0(1)=\tilde{K}_2, \qquad \tilde{g}_0'(1)=0. \tag{6.49}$$

This system fixes $\tilde{K}_2$, and it can be shown from the results for g_1 and $\tilde{p}_1$ above, that

$$\begin{aligned} &\tilde{K}_2 = -\tfrac{3}{4} + \mathrm{O}(\lambda), \quad (\lambda \to 0), \\ &\tilde{K}_2 = \mathrm{O}(\lambda^{1/3}), \qquad (\lambda \to \infty). \end{aligned} \tag{6.50}$$

It can be confirmed that the first result, which gives

$$K = \tfrac{1}{2} - \tfrac{3}{4}\alpha^2 + \ldots \qquad (\lambda \to 0, \alpha \to 0) \tag{6.51}$$

is consistent with the form of (4.9) for $\alpha \ll 1$.

One of the main interests in the results of the analysis for $\lambda \gg 1$ lies in an estimate of the first separation of the flow as α increases from zero. From the above results, and for the profile (6.45), the skin friction at the wall is given by

$$\left.\frac{\partial v}{\partial r}\right|_{x=F} \simeq -1 + 3\alpha\lambda^{1/3}\,\mathrm{Ai}(0)\cos\left(\theta - \frac{\pi}{3}\right), \qquad (1 \ll \lambda \ll \alpha^{-3}),$$

$$(\mathrm{Ai}(0) = 0.3550\ldots). \tag{6.52}$$

The corresponding pressure distribution, from (6.41), (6.22), (6.13) and (6.3) is

$$P = 3\alpha\lambda^{2/3}|\mathrm{Ai}'(0)|\{\cos(\theta - \tfrac{2}{3}\pi) + \tfrac{1}{2}\}, \qquad (1 \ll \lambda \ll \alpha^{-3}). \tag{6.53}$$

The result (6.52) shows that the asymptotic theory for $\lambda \to \infty$ fails when the (small) modulation of the outer cylinder wall is sufficiently large, specifically $\alpha = \mathrm{O}(\lambda^{-1/3})$. Strictly speaking, as α increases from zero, separation will first occur in this new regime, in which it appears that the full boundary-layer equations will govern the flow in a region of width $\mathrm{O}(\lambda^{-1/3})$ near the outer cylinder. Apart from conditions of periodicity, the situation is likely to be similar to that of the perturbed-Poiseuille-flow studies by Smith [9], with the pressure, of $\mathrm{O}(\lambda^{1/3})$, determined as part of the boundary-layer solution. It is hoped to consider this regime in a future paper.

The present theory may still be used to obtain an *approximate* estimate of the first occurrence of separation when $\lambda \gg 1$. According to (6.52) it occurs at $\theta = \pi/3$ when

$$\alpha = \tfrac{1}{3}\lambda^{-1/3}|\mathrm{Ai}(0). \tag{6.54}$$

Here the gap between the cylinders is widening and the pressure is rising from its minimum value

$$P_{\min} = -\tfrac{3}{2}\alpha\lambda^{2/3}|\mathrm{Ai}'(0)| \qquad \text{at} \qquad \theta = \tfrac{5}{3}\pi, \tag{6.55}$$

to its maximum value

$$P_{\max} = \tfrac{9}{2}\alpha\lambda^{2/3}|\mathrm{Ai}'(0)| \qquad \text{at} \qquad \theta = \tfrac{2}{3}\pi. \tag{6.56}$$

This behaviour compares well with the trend of the numerical solution for $\lambda = 100$, $\alpha = 0.1$, shown in Fig. 2; the maximum and minimum values of the pressure given by (6.55) and (6.56) are 2.48 and -0.83 in this case.

References

[1] P.M. Eagles and F.T. Smith, The influence of nonparallelism in channel flow stability, *J. Eng. Math.* 14 (1980) 219–237.

[2] J.R. Bodoia and J.F. Osterle, Finite difference analysis of plane Poiseuille and Couette flow developments, *Appl. Sci. Res.* A10 (1961) 265–276.

[3] J. Paris and S. Whitaker, Confined wakes: a numerical solution of the Navier-Stokes equations, *A.I.Ch.E. Journal* 11 (1965) 1033–1041.

[4] F.G. Blottner, Numerical solution of slender channel laminar flows, *Comp. Meth. in Appl. Mech. & Eng.* 11 (1977) 319–339.

[5] A. Plotkin, Spectral method solutions for some laminar channel flows with separation, *A.I.A.A.* paper no. 82-0258 (A.I.A.A. Aerospace Scientific Meeting, Orlando, Florida) (1982).

[6] R.C. DiPrima and J.T. Stuart, Flow between eccentric rotating cylinders, *J. Lub. Tech. Trans. A.S.M.E.*, Series F, paper no. 72-*Lub. J.* (1972) 266–274.

[7] R.C. DiPrima and J.T. Stuart, Non-local effects in the stability of flow between eccentric rotating cylinders, *J. Fluid Mech.* 54 (1972) 393–415.

[8] P.M. Eagles, J.T. Stuart and R.C. DiPrima, The effects of eccentricity on torque and load in Taylor-vortex flow, *J. Fluid Mech.* 87 (1978) 209–231.

[9] F.T. Smith, Flow through constricted or dilated pipes and channels: Part 1, *Q. J. Mech. Appl. Math.* 29 (1976) 343–364.